Cell Stress and Chaperones (2025) 30:143–159
https://doi.org/10.1016/j.cstres.2025.03.003

Amyloidogenesis promotes HSF1 activity enhancing cell survival during breast cancer metastatic colonization

Natasha Hockaden[1] · Gabi Leriger[1] · John Wang[1] · Haimanti Ray[1] · Sunandan Chakrabarti[1] · Nicholas Downing[1] · Jacob Desmond[2] · David Williams[2] · Peter C. Hollenhorst[1,3,4] · Gregory Longmore[5] · Richard L. Carpenter[1,3,4,*]

Received: 8 November 2024 / Revised: 10 February 2025 / Accepted: 20 March 2025

Abstract

Breast cancer is the most commonly diagnosed cancer among women and the second leading cause of cancer deaths in women. A majority of these breast cancer deaths are due to metastasis, which occurs when primary tumor cells invade into the blood stream to travel and colonize at distant organ sites. Metastatic colonization is the rate-limiting step of metastasis. Heat shock factor 1 (HSF1) is a transcription factor that has been shown to be involved in promoting malignancy with a function in metastatic dissemination due to its contribution to promoting epithelial-to-mesenchymal transition. The role of HSF1 in colonization is unclear. In this study, we observed that HSF1 was essential for metastatic colonization. Consistent with these findings, we also observed that HSF1 was more active in human metastatic tumors compared to primary tumors. HSF1 was also seen to be activated during *in vitro* colony formation, which was accompanied by increases in amyloid beta (Aβ) fibrils, which was also observed in human metastatic tumors. Aβ fibrils led to HSF1 activation and depletion or inhibition of HSF1 led to increases in Aβ fibrils. HSF1 inhibition with small molecule inhibitors suppressed *in vitro* colony formation and mammosphere growth of metastatic breast cancer cells. These results suggest that colonization increases Aβ fibril formation that subsequently activates HSF1 as a cell survival mechanism that is essential for metastatic initiation and outgrowth.

Keywords HSF1 · Breast cancer · Metastasis · Amyloid beta · Colonization

Introduction

Breast cancer is the most commonly diagnosed cancer in women around the world.[1,2] Recent trends indicate a troubling increase in breast cancer incidence and the current 5-year survival rate is 99%.[2] However, this 5-year survival rate drops precipitously to 32% for patients with distant stage disease, reflecting that the majority of patients that die from breast cancer is caused by distant metastasis.[2] One in eight women is at risk for developing invasive breast cancer, and about 20–30% of women with early stage breast cancer will develop metastases.[1] Furthermore, patients with triple-negative breast cancer (TNBC) are typically diagnosed at later stages, at earlier ages, and have fewer effective therapies.[3,4] The vast majority of metastatic breast cancer patients are managed with palliative, non-curative treatment such as radiation and/or chemotherapy (56% of patients) with 26% of patients receiving no treatment at all.[5]

Abbreviations: Aβ, Amyloid beta; DAST, Diethylaminosulfur trifluoride; DDQ, 2,3-Dichloro-5,6-dicyano-1,4-benzoquinone; EMT, Epithelial-to-mesenchymal transition; HSP, Heat shock protein; PPh_3, Triphenylphosphine; MET, Mesenchymal-to-epithelial transition; TNBC, Triple-negative breast cancer; XtalFluor-E, (Diethylamino)difluorosulfonium tetrafluoroborate

* Richard L. Carpenter
richcarp@iu.edu

[1] Medical Sciences, Indiana University, Bloomington, IN 47405

[2] Department of Chemistry, Indiana University, Bloomington, IN 47405

[3] Department of Biochemistry and Molecular Biology, Indiana University School of Medicine, Indianapolis, IN 46202

[4] Simon Comprehensive Cancer Center, Indiana University School of Medicine, Indianapolis, IN 46202

[5] Department of Cell Biology and Physiology, Washington University School of Medicine, St. Louis, MO 63110.

Published online: 25 March 2025

The process of metastasis first involves the primary tumor cells invading healthy tissue surrounding the primary tumor and intravasation into the circulation (dissemination). After being transported to distant organs by the circulation, cells will extravasate and colonize new tumors at distant organ sites.[6,7] Breast cancer frequently metastasizes to the liver, lungs, and brain but most often spreads to bones.[7,8] Metastasis is a highly inefficient process with an estimated 99.98% of disseminated cancer cells dying before a metastasis forms.[7] Dissemination[9] and extravasation[10] are rather efficient processes and most cell death occurs after extravasation and during colonization. Only a small fraction (< 3%) of cells survive to form micrometastases with a lower rate of formation for larger, established metastatic lesions.[10,11] Cancer cells face many stressors during metastasis, especially during the rate-limiting step of colonization, wherein cells must adapt to survive in isolation within a new tissue environment.

Heat shock factor 1 (HSF1) acts as the master regulator of the heat shock response by inducing the expression of heat shock protein (HSP) genes in response to elevated temperatures. Upon heat stress, cytoplasmic HSF1 monomers are released from sequestration by HSPs that are siphoned away to assist in the maintenance of the proteome.[12] After release by HSPs, HSF1 enters the nucleus, undergoes trimerization, phosphorylation, and DNA binding to heat shock elements that ultimately promote expression of HSP genes to further manage the stress.[12] HSF1 has been shown to play a significant role in breast and other cancers[12,13] with this role being partially composed of its role in managing proteostasis. HSF1 was shown to be critical to suppressing toxic levels of amyloidogenesis in cancer cells as a means of cell survival.[14] HSF1 expression and activity have been associated with poor patient outcomes in breast cancer.[15–19] HSF1 has also been linked to TNBC as HSF1 activity was shown to be highest in TNBC relative to other subtypes.[17]

Elegant studies by the Lindquist lab found that HSF1 appears to localize and regulate a unique set of genes in cancer cells distinct from its binding under heat stress.[18] The composition of the genes HSF1 regulates in cancer cells was highly varied and not specific to proteostasis, suggesting HSF1 serves pleiotropic roles in tumors. This finding has been validated by many studies showing HSF1 plays a role in a variety of cancer processes, including cancer cell metabolism,[20,21] DNA repair,[22] cell survival,[23,24] and epithelial-to-mesenchymal transition (EMT),[25–29] among many others. HSF1 has previously been linked to metastasis.[13] However, these links have largely been related to migration, invasion, and EMT that contribute to dissemination.[25–31] A role for HSF1 in other aspects of metastasis is unclear. Here we observed that metastatic colonization is severely compromised without HSF1. This is accompanied by increased activation of HSF1 in metastatic tumors from patients that were consistent using *in vitro* models of colonization. We found that amyloidogenesis was upregulated during colonization *in vitro* and in metastatic tumors from patients also showing evidence of more amyloid fibrils compared to primary tumors. Generation of amyloid fibrils led to HSF1 activation and loss of HSF1 increased amyloid fibril formation. Small molecule inhibition of HSF1 successfully repressed *in vitro* colonization as well as mammosphere growth. These results suggest amyloid fibrils are generated during colonization and that HSF1 is necessary for the cellular response to these aggregate fibrils to maintain cell survival for subsequent colonization and outgrowth.

Results

Loss of HSF1 reduces metastatic breast tumor formation

HSF1 activity has been associated with worse overall survival and worse metastasis-free survival of breast cancer patients.[15,17,18] We have previously found a mechanism for HSF1 to promote EMT,[25] which could possibly account for the association of HSF1 with metastasis. However, we have also observed that HSF1 is more active in bone and brain metastasis-derived MDA-MB-231 breast cancer cells compared to parental cells,[15] suggesting HSF1 may also play a functional role in cells after metastatic dissemination. To test this, MDA-MB-231 breast cancer cells were engineered to have shRNA-mediated stable HSF1 knockdown (Figure 1(a)). HSF1 knockdown MDA-MB-231 cells were observed to have similar proliferation rates (Figure 1(b)), however, were seen to have a significantly decreased colony forming ability compared to control MDA-MB-231 cells (Figure 1(c) and (d)). Therefore, we next tested whether these cells have differences in metastasis after dissemination intracardially injecting control or HSF1 knockdown cells in nude mice to bypass the step of dissemination and tracked by bioluminescence over 30 days (Figure 1(e)). Bone metastases were clearly visible in leg bones of mice injected with control and HSF1 knockdown cells by histology (Figure 1(f)). While some legs from mice injected with HSF1 knockdown cells showed some visible tumors, there were fewer mice with visible tumors injected with HSF1 knockdown cells compared to mice injected with control cells. These tumors stain positive for anti-HLA-C, indicating they are of human origin (Supplementary Figure 1(a)). Mice injected with

cells lacking HSF1 showed a significantly reduced metastatic burden, indicating a lower number of total metastases detected, compared to control cells as measured with bioluminescent imaging (Figure 1(g)). The size of metastases that developed was estimated by the average flux of tumors via bioluminescence. Metastases in mice injected with HSF1 knockdown cells were significantly smaller compared to mice injected with control cells (Supplementary Figure 1(b)). Consistent with these data, mice injected with control cells showed significantly worse metastasis-free survival (Figure 1(h)). Since intracardiac injection bypasses the dissemination step of metastasis, these data suggest that HSF1 is essential for metastatic colonization and that HSF1 is important for multiple aspects of the metastatic process rather than invasion or dissemination only.

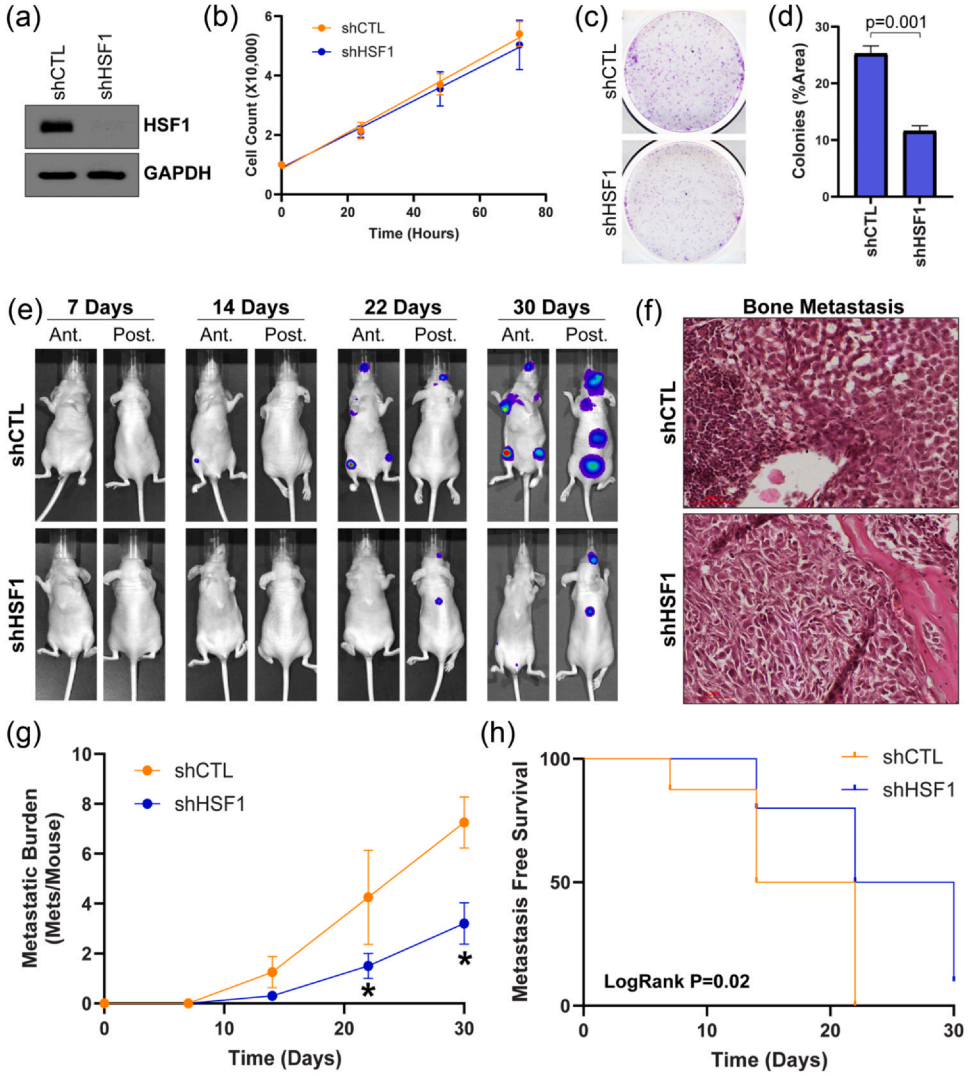

Fig. 1 HSF1 is required for metastatic colonization. (a) MDA-MB-231 cells with stable expression of control (shCTL) or HSF1 shRNA (shHSF1) were generated and total protein was subjected to immunoblotting with the indicated antibodies. (b) Control (shCTL) and HSF1 knockdown (shHSF1) MDA-MB-231 cells were subjected to a proliferation assay over 72 h. (c) and (d) Control (shCTL) and HSF1 knockdown (shHSF1) MDA-MB-231 cells were subjected to a clonogenic growth assay (c) and colonies were quantified by measuring total area of colonies (d). Student *t*-test was used to compare colony area, and experiments were completed in biological triplicate. (e-h) Control (shCTL; n = 8) and HSF1 knockdown (shHSF1; n = 9) MDA-MB-231 cells underwent intracardiac injection into nude mice and tumors were tracked by bioluminescence over 30 days (e). Representative H&E stain of a femur from mice injected with shCTL and shHSF1 cells is shown (f). Metastatic tumor burden (g) and metastasis-free survival (h) of mice from (e) are plotted. Two-way ANOVA with Tukey's post hoc test was performed in (g); *indicates significant differences between shCTL and shHSF1 groups. Log rank test was performed in (h) for comparison between shCTL and shHSF1 groups. Abbreviations used: Ant, anterior view; Post, posterior view; H&E, hematoxylin & eosin; ANOVA, analysis of variance.

HSF1 is activated in metastatic tumors and during *in vitro* colony formation

If HSF1 is required for metastatic colonization, we hypothesized that HSF1 may show increased activation in metastatic tumors compared to primary tumor counterparts. We first tested whether the HSF1 activity signature[17] was different between primary tumors and metastatic tumors using TNMplot.[32] These results indicated an increase in HSF1 activity in primary tumors compared to normal breast tissue and a further increase in HSF1 activity in metastatic tumors compared to primary tumors (Kruskall–Wallis $P = 8.2e\text{-}48$) (Figure 2(a)). We next analyzed a small cohort (n = 13) of patient tumors wherein the primary tumor from the breast tissue and matched metastatic tumors from bone metastases were available. Immunohistochemistry (IHC) was performed using antibodies for the active phosphorylated (S326) form of HSF1 (Figure 2(b)). This staining indicated that most of these patients tumors had higher HSF1 activity in their bone metastases compared to their primary tumors, which was significant when analyzed with a paired *t*-test (Figure 2(c)).

We have previously observed that loss of HSF1 impairs *in vitro* colony formation.[15,25] These results, along with the current study showing *in vivo* metastatic formation requires HSF1, suggest HSF1 is likely activated during *in vitro* colonization. To test this, breast cancer cells were subjected to *in vitro* clonogenic growth (Figure 3(a)–(c)), and these lysates were collected after colony formation for immunoblotting for the active form of HSF1 (p-S326). We included two often used TNBC cell lines in MDA-MB-468 and MDA-MB-231 cells. We additionally added MDA-MB-231-BoM cells, which were previously generated by collecting bone metastases derived from the injection of MDA-MB-231 cells and re-injecting these cells to again collect bone metastases through several rounds.[33] The end result is a markedly metastatic MDA-MB-231-derived cell line that has a high preference for bone metastasis. All three cell lines showed greater active HSF1 in colonies compared to cells undergoing normal growth at approximately 80% confluency (Figure 3(d)–(f)). Considering HSF1 has previously been linked to mitosis,[34] it is possible the role of HSF1 in the cell cycle could contribute to results in Figure 3. However, we did observe greater effects of HSF1 loss on colony formation (Figure 1(c) and (d)) than proliferation (Figure 1(b)). Therefore, these results suggest that HSF1 is activated during *in vitro* colony formation and *in vivo* metastatic colonization, as metastatic tumors from patients also had increased active HSF1.

Amyloidogenesis increases during colony formation and correlates with HSF1 activation

Considering our observations that HSF1 is required for metastatic colonization (Figure 1) and that HSF1 is activated in metastatic tumors (Figure 2) and during *in vitro* colony formation (Figure 3), we next sought to identify potential triggers for the activation of HSF1. The physiological activation of HSF1 is driven by imbalances in proteostasis, which classically occurs with heat stress.[12] Amyloidogenesis, or the formation of amyloid beta (Aβ)-derived oligomers that lead to complex fibril aggregates, is a tumor-suppressive process toxic to cells that HSF1 can suppress for the benefit of cancer cell survival and growth.[14] We next assessed

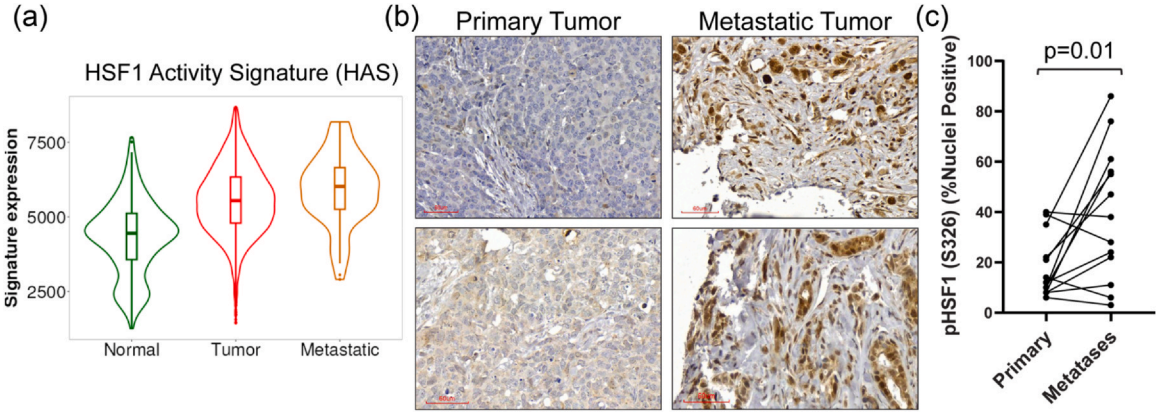

Fig. 2 HSF1 is more active in metastatic tumors compared to primary tumors. (a) The HAS was plotted in normal, primary tumors, and metastatic breast tumors using TNMplot. Kruskall–Wallis test was performed for differences between groups. (b) and (c) A cohort of 13 primary along with matched bone metastases from human breast cancer patients were subjected to IHC with antibodies for active HSF1 (pS326) (b). Staining was quantified using QuPath and the percent of cells with positive nuclear staining was compared using a paired *t*-test (c). Abbreviations used: HSF1, heat shock factor 1; IHC, immunohistochemistry.

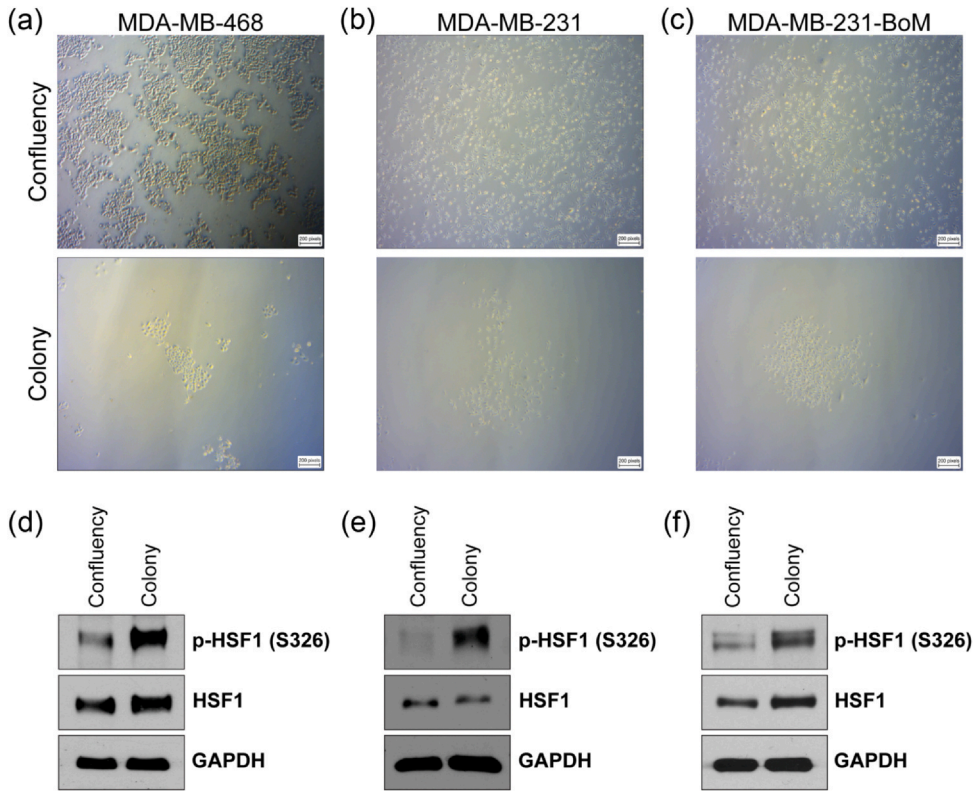

Fig. 3 HSF1 is activated during *in vitro* colony formation. (a–c) Representative images of cells growing toward confluency (approximately 70–90% confluent) and colonies formed during clonogenic growth assays for MDA-MB-468 (a), MDA-MB-231 (b), and MDA-MB-231-BoM (c) cells. (d)–(f) Total protein from cells growing toward confluency or cells from colony formation in (a)–(c) were subjected to immunoblotting with the indicated antibodies for MDA-MB-468 (d), MDA-MB-231 (e), and MDA-MB-231-BoM (f) cells. Experiments were completed in biological triplicate. Abbreviation used: HSF1, heat shock factor 1.

whether levels of Aβ fibrils also change during *in vitro* colony formation. Using a previously characterized conformation-dependent antibody for Aβ fibrils, OC,[14,35] we detected an increase in Aβ fibrils using an ELISA assay in cells undergoing *in vitro* colony formation compared to control cells growing under normal growth conditions to confluency (Figure 4(a) and (b)). This correlated with the increase in active HSF1 seen in cells undergoing the same colony formation process (Figure 3(d)–(f)). To determine whether experimental induction of amyloidogenesis would increase levels of active HSF1, we transfected cells with Aβ (1-42), a peptide that is a fragment of Aβ that has previously been shown to promote Aβ fibril formation.[36] Transfection of Aβ (1-42) for 8–24 h was found to promote significant increases in Aβ fibril formation (Figure 4(c) and (d)). Fibril formation peaked at 8 h with subsequent time points showing decreased fibrils. Transfecting cells with Aβ (1-42) for 8 h led to increased levels of active HSF1 (p-S326) (Figure 4(e) and (f)). Levels of active HSF1 peaked at 8 h and decreased at later time points, similar to Aβ fibrils. These results suggest induction of Aβ fibril formation leads to HSF1 activation. HSF1 responds to this Aβ accumulation by decreasing fibrils to enhance cell survival.

Amyloid fibrils in primary and metastatic breast tumors correlates with active HSF1

In vitro colonization led to increases in Aβ fibril formation (Figure 4). Therefore, we next tested whether these fibrils are also present and associated with active HSF1 in human breast tumors. Unfortunately, there was not enough tissue material from the cohort of matched primary and metastatic tumors in Figure 2, to assess fibril formation. Therefore, we analyzed independent cohorts of primary tumors (n = 112) and metastatic tumors (n = 141) by IHC with antibodies for Aβ fibrils (OC) and active HSF1 (p-S326) (Figure 5(a)). While there were significantly more Aβ fibrils in tumors with high HSF1 activity (Supplementary Figure 2(a)), there was not a significant Pearson correlation between fibrils and active HSF1 in primary tumors (Figure 5(b)). However, in metastatic tumors, there were significantly more Aβ fibrils in high active HSF1 tumors (Supplementary Figure 2(b)) and there was a significant

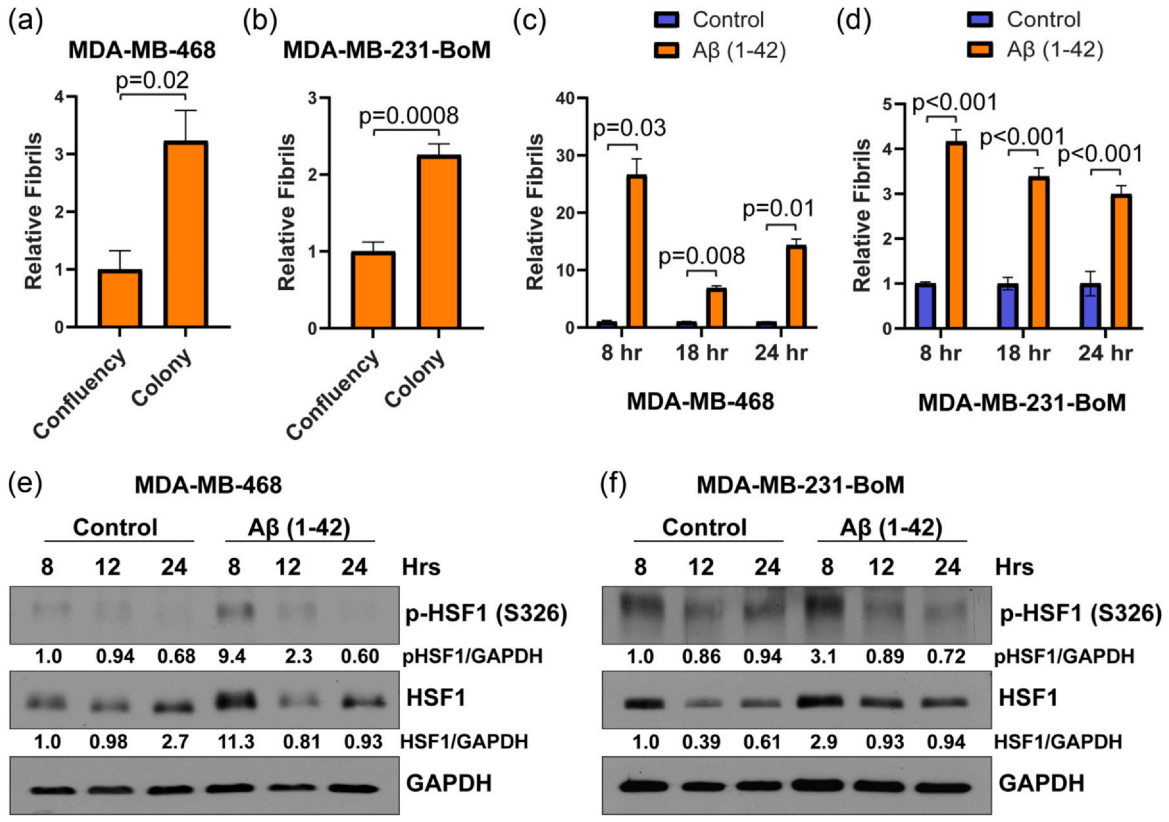

Fig. 4 Aβ fibrils form during colony formation and promote HSF1 activation. (a) and (b) MDA-MB-468 (a) and MDA-MB-231-BoM (b) cells were grown toward confluency (~80 confluent) or in a colony formation assay. Insoluble protein was collected from the cells under these conditions and was subjected to an ELISA for Aβ fibrils (OC antibody). These experiments were completed with at least biological triplicates. (c–f) MDA-MB-468 (c, e) and MDA-MB-231-BoM (d, f) cells were transfected with a control peptide or Aβ (1–42) peptide for the indicated time points. Insoluble protein was collected and subjected to an ELISA for Aβ fibrils (OC antibody) (c and d) or to immunoblotting with the indicated antibodies (e and f). Experiments were completed with biological triplicates. Abbreviation used: HSF1, heat shock factor 1.

positive Pearson correlation between Aβ fibrils and active HSF1 (Figure 5(c)). This suggests that HSF1 activity in metastatic tumors may be more driven by Aβ fibrils compared to primary tumors. Consistent with this hypothesis and with data in Figure 2, there was significantly more active HSF1 in the independent metastatic cohort compared to the primary tumor cohort (Figure 5(d)). Furthermore, there were significantly more Aβ fibrils in the metastatic cohort compared to the primary tumor cohort (Figure 5(e)). These findings would also predict that the metastases observed *in vivo* after intracardiac injection (Figure 1) would have more Aβ fibrils compared to primary tumors from the same cell line. To test this, we compared levels of Aβ fibrils by IHC (OC Ab) in the bone metastases to tumors grown in the mammary fat pad (Figure 5(f)). We found these metastases had significantly more Aβ fibrils compared to tumors grown in the mammary fat pad (Figure 5(g)), consistent with the hypothesis that Aβ fibrils form during the process of colonization leading to HSF1 activation and cell survival.

Knockdown or inhibition of HSF1 increases amyloidogenesis

Considering our observation that Aβ (1-42)-induced fibrils promoted HSF1 activation (Figure 4) and that HSF1 activation was correlated with Aβ fibrils in patient tumors (Figure 5), we next assessed whether altering HSF1 leads to changes in Aβ fibrils. MDA-MB-231 and MDA-MB-231-BoM were both subjected to transient HSF1 knockdown using siRNA, which was observed to significantly increase Aβ fibrils compared to control siRNA (Figure 6(a) and (b)). Small molecular inhibitors of HSF1 were next tested and included the recently developed SISU-102 (also known as DTHIB),[37] KRIBB11,[38] and $I_{HSF}115$.[39] These inhibitors all have different modes of action to inhibit HSF1. SISU-102 was found by screening for compounds that bind the HSF1 DNA binding domain and, upon binding, leads to destabilization and degradation of nuclear active HSF1, thereby reducing transcriptional activity of HSF1.[37] KRIBB11 is reported to bind the HSF1 transactivation domain to block recruitment of CDK9 for gene

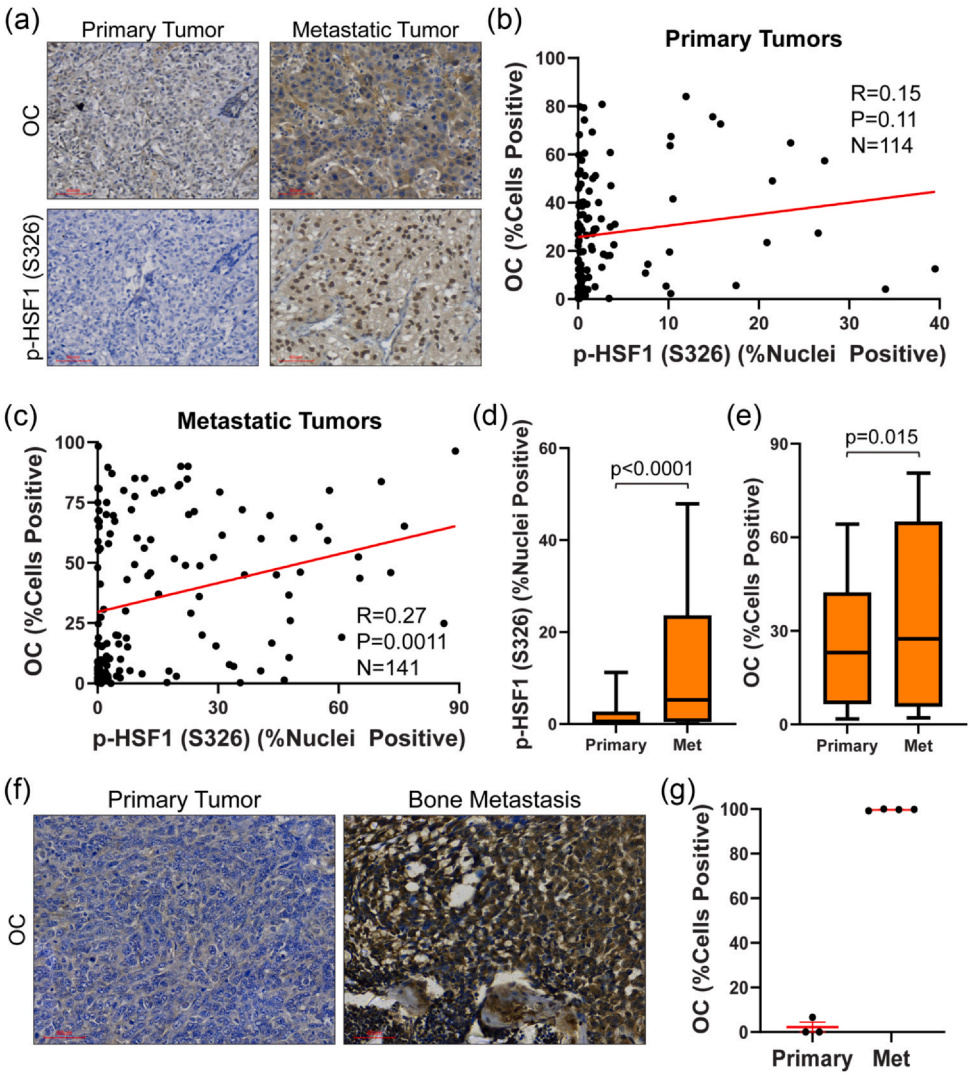

Fig. 5 Aβ fibrils are correlated with active HSF1 in metastatic tumors. (a) A cohort of 114 primary tumors from human patients and an independent cohort of 141 metastatic tumors from human patients were subjected to IHC with the indicated antibodies. (b) and (c) The percent cells positive for OC and the percent nuclei positive for active HSF1 (pS326) were quantified using QuPath and subjected to a Pearson correlation in primary (b) and metastatic (c) tumors. (d) and (e) The percent nuclei positive for active HSF1 (pS326) (d) and the percent cells positive for OC (e) were compared between the primary (n = 114) and independent metastatic (n = 141) tumor cohorts. Independent *t*-test was used to test for significance. (f) and (g) Primary tumors from MDA-MB-231 shCTL cells were grown in the mammary fat pad or bone metastases after intracardiac injection of these cells (Figure 1) were subjected to IHC for Aβ fibrils (OC antibody) (f), which was quantified using QuPath for these primary and bone metastases (g). Abbreviation used: HSF1, heat shock factor 1.

transactivation.[38] $I_{HSF}115$ binds the HSF1 DNA binding domain and blocks gene activation but does not disrupt DNA binding.[39] To first test for a dose range that reduces HSF1 activity, all three compounds were added to cells, and expression of the HSF1 direct target HSP27 was assessed to ascertain the dose at which HSP27 decreased compared to control. Both SISU-102 and KRIBB11 were found to significantly reduce HSP27 using doses of 5–10 μM (Figure 6(c) and (d)) whereas $I_{HSF}115$ was not observed to reduce HSP27 within the dose ranges tested (Supplementary Figure 3(a)). These inhibitors were next added to stable MDA-MB-231 shCTL and shHSF1 cells and assessed cell proliferation to test for HSF1 selectivity. Both SISU-102 and $I_{HSF}115$ significantly reduced cell counts in shCTL cells after 48 h whereas the effect of KRIBB11 did not reach significance (Supplementary Figure 3(b)–(d)). SISU-102 did not significantly reduce counts of shHSF1 cells compared to the vehicle, suggesting SISU-102 is likely dependent on HSF1 for its effects (Supplementary Figure 3(b)–(d)). Due to their impact on HSF1 activity, both SISU-102 and KRIBB11 were administered to

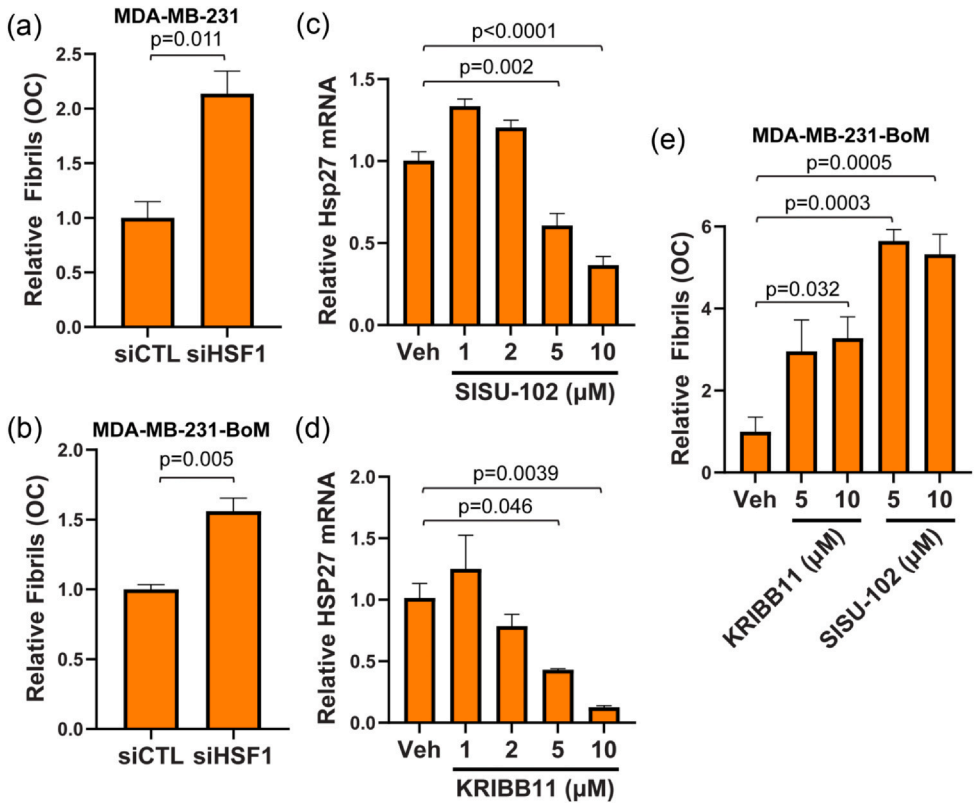

Fig. 6 Inhibition of HSF1 increases Aβ fibrils. (a) and (b) MDA-MB-231 (a) or MDA-MB-231-BoM (b) cells were transfected with control (CTL) or HSF1 siRNA for 48 h. The insoluble fraction of these cells was collected and subjected to an ELISA for Aβ fibrils (OC antibody). Significant differences were compared using an independent *t*-test. (c) and (d) MDA-MB-231 cells were treated with SISU-102 (c) or KRIBB11 (d) at the indicated doses for 24 h. Total RNA was collected and subjected to RT-qPCR for primers to HSP27. (e) MDA-MB-231-BoM cells were treated with the indicated inhibitors at the indicated doses for 24 h. The insoluble fraction of the cells was collected and subjected to an ELISA for Aβ fibrils (OC antibody). Comparisons were made using a one-way ANOVA with Tukey's post-hoc test. All experiments were completed with at least three biological replicates. Abbreviation used: HSF1, heat shock factor 1; ANOVA, analysis of variance.

MDA-MB-231-BoM cells and assessed for Aβ fibril generation. While KRIBB11 induced a minor increase in fibrils, SISU-102 was found to induce a significant increase in fibrils (Figure 6(e)). These results suggest that suppression of HSF1 leads to an increase in Aβ fibril formation.

Inhibition of HSF1 reduces colony and mammosphere formation

Because SISU-102 and KRIBB11 both showed an ability to decrease HSF1 activity, these inhibitors were next used to test whether HSF1 inhibition affects *in vitro* colony formation. MDA-MB-468 (Figure 7(a) and (b)), MDA-MB-231 (Figure 7(c) and (d)), and MDA-MB-231-BoM (Figure 7(e) and (f)) cells were subjected to clonogenic growth in the presence or absence of these HSF1 inhibitors. Results indicated that all cell lines tested were sensitive to HSF1 inhibition with a significant reduction in colony formation. In total, these results suggest that HSF1 could serve as a therapeutic target to suppress metastasis. To further understand the potential of HSF1 inhibition as a therapeutic approach, these inhibitors were tested using three-dimensional spheroids, often referred to as mammospheres. Three-dimensional growth is considered a better predictor of *in vivo* therapeutic response to inhibitors than standard two-dimensional cell culture growth.[40] MDA-MB-468 (Figure 8(a) and (b)) and MDA-MB-231-BoM (Figure 8(c) and (d)) cells, which are capable of growing under low-attachment mammosphere conditions, were subjected to mammosphere growth with or without SISU-102 and KRIBB11. Mammosphere growth was found to be significantly impaired in the presence of either HSF1 inhibitor. Together, these data suggest that HSF1 is critical during *in vitro* and *in vivo* colonization by suppressing the accumulation of toxic protein aggregates, and inhibition of HSF1 may be a viable strategy to reduce colonization and metastasis.

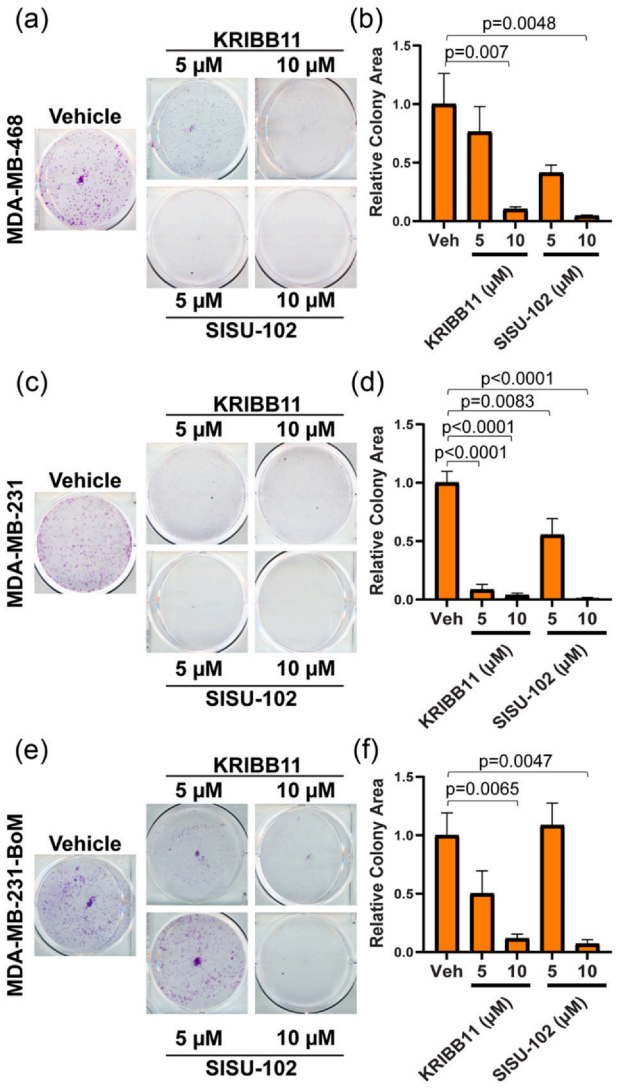

Fig. 7 HSF1 inhibition suppresses *in vitro* colony growth. (a)–(f) MDA-MB-468 (a) and (b), MDA-MB-231 (c) and (d), and MDA-MB-231-BoM (e) and (f) were subjected to *in vitro* colony growth assays in the presence of either vehicle, KRIBB11, or SISU-102 at the indicated doses for 7–10 days. Wells were quantified using ImageJ to measure the area covered by colonies and normalized relative to the vehicle. One-way ANOVA with Tukey's post-hoc test was used to compare groups within each cell line. All experiments were completed with at least three biological replicates. Abbreviation used: HSF1, heat shock factor 1; ANOVA, analysis of variance.

Discussion

HSF1 has been shown to have pleiotropic roles in cancer over the last few decades.[12,13] Many of the discovered roles for HSF1 in tumor biology largely support the progression of tumors from early to late stages, which is evident as HSF1 activity has been shown to increase with later-staged tumors.[19] HSF1 can promote the progression of tumors toward higher stages through its pleiotropic functions in tumors including roles in metabolism,[20,21] increased cell mobility, EMT,[25–31] and stemness[15,41–47] among many of the other functions HSF1 contributes to cancer cells. There has been clear evidence of a role for HSF1 in metastasis that includes functional studies wherein metastasis was compromised without HSF1 or HSF1 itself was associated with metastasis as an outcome.[13,17,18,48] However, many of these results could be attributed to the role of HSF1 in metastatic dissemination since HSF1 has been shown to promote migration, invasion, and EMT.[25–31] The current study bypassed the dissemination step to inject cells directly into the circulation to assess any potential roles for HSF1 in the later stages of metastasis, primarily metastatic colonization. Thus, the previous clinical associations made between HSF1 and overall survival and metastasis-free survival likely include roles for HSF1 in metastatic dissemination but also roles during metastatic colonization.

Imbalances in proteostasis, or protein homeostasis, is a characteristic of cancer cells that is derived from tumor tissues and cancer cell-intrinsic features. Tumor tissue is often acidic and hypoxic, creating a stressful environment for cancer cells. Cancer cells are frequently characterized by an upregulation of mTORC1 signaling that leads to enhanced translation and protein biosynthesis, aneuploidy has been shown to promote proteotoxic stress, and oxidative stress is higher in cancer cells that leads to damaged proteins.[49] Detection of amyloid fibrils in cancer cells has been detected and HSF1 has been shown to suppress amyloidogenesis as a cell survival mechanism.[14] The current study supports these findings and extends them to observe increased amyloidogenesis during *in vitro* and *in vivo* colonization. It is possible that active proliferation also leads to amyloidogenesis and contributes to these results. While HSF1 has been linked to proliferation,[34,50] we observed greater effects of HSF1 loss on colonization than proliferation (Figure 1). The contribution to mitosis by HSF1 would certainly impact metastatic outgrowth after initiation and could have contributed to the results of this study. Consequently, we conclude that these findings suggest a model whereby colonization induces proteotoxic stress to cancer cells, promoting the formation of amyloid fibrils that, in turn, activate HSF1 as a survival mechanism.

HSF1 activation in response to proteotoxic stress during colonization would predict that HSF1 activity may be the strongest during early colonization at the stage of micro-metastases. This prediction would also fit with the known role of HSF1 in promoting EMT.[25–31] EMT can enable primary tumor cells the capability for mobility and anchorage-independent growth. After colonizing at a new organ site, cells undergo the reverse

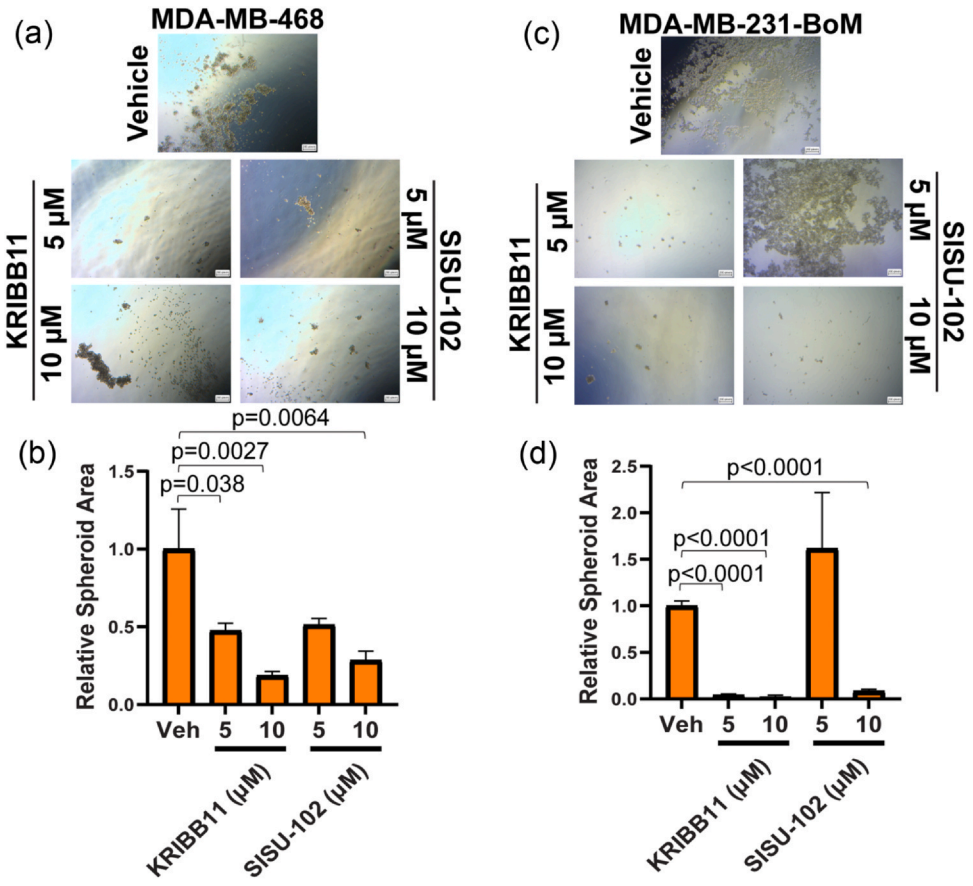

Fig. 8 HSF1 inhibition suppresses mammosphere growth. (a)–(d) MDA-MB-468 (a) and (b) and MDA-MB-231-BoM (c) and (d) cells were subjected to mammosphere growth in the presence of vehicle, KRIBB11, or SISU-102 at the indicated doses for 7–14 days with supplementation of media every two days. The sum of the area of each well-containing mammospheres was quantified using ImageJ and normalized relative to the vehicle. One-way ANOVA with Tukey's post-hoc test was used to compare groups within each cell line. All experiments were completed with at least three biological replicates. Abbreviation used: HSF1, heat shock factor 1; ANOVA, analysis of variance.

process called mesenchymal-to-epithelial transition, leading to a tumor with many cells that retain an epithelial identity. This model would possibly predict that HSF1 could be downregulated at some point after colonization and result in some variance for HSF1 activation depending on when metastatic tumor samples were analyzed. It is unclear at which stage the patient metastatic tumor samples in the current study were collected in relation to when these tumors underwent colonization. These samples indicated a statistically significant increase in active HSF1 in metastatic tumors but there was variance in these cohorts. There is significant variance in HSF1 activation across primary tumors but HSF1 active tumors are more likely to metastasize.[17–19] Thus, metastatic tumors may also have a similar variance such that tumor cells leading up to EMT that are anticipating movement utilize HSF1 to promote EMT and suppress proteotoxic stresses that occur during the process. However, inducible knockdown of HSF1 following colonization of brain metastases from lung tumors did result in the reduction of growth,[48] suggesting that HSF1 is also important after successful colonization. Future studies are underway to assess HSF1 across populations of metastatic tumors to understand the variance of HSF1 activation in post-metastatic tumors.

Similar to EMT, HSF1 has also been shown to promote the cancer stem cell population,[15,37,42–47] which plays a role in metastasis and colonization.[51] Evidence indicates that depletion of HSF1 suppresses the cancer stem cell population.[15,37,42–47] The molecular mechanisms for how HSF1 regulates cancer stem cells remain unclear, but it does appear HSF1 is critical for this population in several cancer types. The cancer stem cell population is thought to provide a cell state that enables better survival and self-renewal,[51] both of which would

be highly beneficial during metastasis. While we utilized tumor spheroids in the current study to have a better estimate of *in vivo* therapeutic response,[40] the response of HSF1 inhibition suppressing spheroid growth is consistent with our previous data indicating HSF1 is more active in spheroids.[15] While clear links between EMT and cancer stem cells remain elusive,[52] HSF1 does seem to be important to the EMT process in cancer cells and the maintenance of the cancer stem cell state. An additional consideration is that HSF1 activity in cancer cell lines has heterogeneity such that the cells with high HSF1 activity are the cells with metastatic potential as they could be driving EMT and/or cancer stem state in a subpopulation of cells, consistent with observations that HSF1 activity is higher in cells sorted with cancer stem markers.[46] Whether that means there is also increased amyloidogenesis in these subpopulations is unclear. Consequently, the role of HSF1 to support these processes and cell states likely contributes to the role of HSF1 in metastatic colonization.

From a therapeutic perspective, targeting HSF1 presents a promising strategy for managing metastases. The small molecule KRIBB11, which binds to the transactivation domain of HSF1, impedes the recruitment of p-TEFb and transcription elongation of HSF1-bound genes.[38] Although KRIBB11 alone showed limited efficacy in reducing tumor volume in some studies, its potential is enhanced when used in combination with other inhibitors such as inhibitors targeting AKT.[15] Notably, KRIBB11 has demonstrated significant tumor growth reduction in preclinical models and has shown effectiveness in overcoming resistance to proteasome inhibitors like bortezomib.[37] Conversely, SISU-102 (also known as DTHIB) targets the DNA-binding domain of HSF1, stimulates nuclear degradation of HSF1, and has proven to be effective in reducing colony formation and tumor size in prostate cancer models.[37] SISU-102 exhibits good specificity with low toxicity to normal tissues, suggesting its potential as a viable therapeutic agent.[37] $I_{HSF}115$ reportedly binds the DNA binding domain of HSF1, it does not alter HSF1 binding but rather affects HSF1 interaction with ATF1.[39] While we did not observe any effect of $I_{HSF}115$ in our system, HSF1 may utilize other partners aside from ATF1 that are unaffected by this compound in the chosen cell lines and systems. Another compound that is reportedly an "HSF1 pathway" inhibitor is NXP800.[53,54] NXP800 was introduced in recent years and is currently in clinical trials for cholangiocarcinoma (NCT06420349) and ovarian cancer (NCT05226507) patients. However, recent studies appear to indicate this compound is an agonist for GCN2 in the integrated stress response pathway rather than directly targeting HSF1[55] even though the compound was initially identified through screening of compounds that suppress HSF1 activity.[53]

Conclusion

This study indicates that HSF1 plays a larger role in cancer metastasis than previously recognized and is essential for metastatic colonization. Furthermore, we observed greater HSF1 activation in metastatic tumors compared to primary tumors and found HSF1 to be activated by colonization *in vitro*. We also observed the generation of Aβ fibrils during *in vitro* colonization and in metastatic tumors and provided evidence that these fibrils can lead to the activation of HSF1. Consistent with this, depletion or inhibition of HSF1 led to increased Aβ fibril formation, suggesting HSF1 is activated during colonization to enhance cell survival to attenuate rising aggregate formation. Targeting HSF1 through specific inhibitors like KRIBB11 and SISU-102 offers a promising approach to manage metastatic cancer and enhance therapeutic outcomes. Future research should focus on optimizing these inhibitors toward increased potency for clinical applications.

Materials and methods

Cell culture, materials, and lentiviral transduction

MDA-MB-468 cells were obtained from ATCC (468: HTB-132, RRID:CVCL_0419). MDA-MB-231 and MDA-MB-231-BoM were a generous gift from Dr Joan Massague at Memorial Sloan Kettering.[33,56] Cells were maintained at 37 °C in 5% CO_2 using DMEM (Gibco #10-013-CV) and were supplemented with 10% fetal bovine serum (Corning #35-011-CV) and 1% penicillin/streptomycin (Gibco #15140-122). Cells were tested monthly for Mycoplasma contamination using MycoAlert kit (Lonza #LT07-218). HSF1 inhibitor treatments were performed with KRIBB11 (Cayman Chemical, 342639-96-7) and SISU-102 (Cayman Chemical, 897326-30-6), stock aliquots were made using dimethyl sulfoxide and stored at −20 °C until use. Lentiviral plasmids carrying control (5'-ACCTAAGGTTAAGTCGCCCTCG-3') or HSF1 (5'-TGCCCAAGTACTTCAAGCACAA-3') shRNA were synthesized by VectorBuilder using miR-30-driven promoter. Lentiviruses were generated using 3rd generation packaging plasmids in HEK293FT (Invitrogen; RRID:CVCL_6911) cells. Virus soup was added to target cells that then underwent selection with puromycin followed by clonal selection in 96-well plates.

Immunoblotting

Immunoblotting was performed using standard sodium dodecyl sulfate polyacrylamide gel electrophoresis techniques with RIPA buffer (50 mM Tris, 150 mM NaCl, 1 mM EDTA, 1% NP-40, 1% sodium deoxycholate, 1% SDS) used to lyse cells as described previously.[57] Antibodies used for immunoblotting included GAPDH (Cell Signaling Technology 2118S, RRID:AB_561053), P-HSF1 (S326) (Abcam EP1713Y, RRID: AB_1310328), and HSF1 (Cell Signaling Technology 4356S, RRID:AB_2120258).

Cell proliferation and colony assays

Cell proliferation was assessed by seeding 10,000 cells into 12-well plates. Cells were trypsinized at 24, 48, and 72 h after seeding and counted to identify increases in cell proliferation over 72 h. For *in vitro* anchorage-dependent colony formation, cells were plated at 1.05 cells/mm2 of cell culture dish area (2000 cells/well of a 6-well plate). Cells were then grown for 6–10 days, depending on the cell line. At the conclusion of the assay, wells were fixed and stained using crystal violet solution with 2% crystal violet with 20% ethanol. Colonies were quantified using ImageJ to measure the area of wells containing colonies. When collecting cells for downstream analyses after colony formation, we used multiple plates to collect enough cells to acquire the appropriate amount of protein needed. Cells were washed in phosphate buffered saline and scraped before being lysed using buffers necessary for the downstream application such as immunoblotting or ELISA for Aβ fibrils.

Animal studies

All animal studies were performed under an approved institutional animal care and use committee protocol on the Indiana University-Bloomington campus (Bloomington, IN). Control (n = 8) or HSF1 knockdown (n = 9) MDA-MB-231 cells (1e5) were injected into the left ventricle of 4-week-old female *nu/nu* mice and metastatic tumor development was monitored by bioluminescence using an IVIS Lumina X5 weekly. Once mice reached humane endpoints, all animals were euthanized. Metastatic tumor burden was calculated by counting the number of unique tumors per mouse and averaged for mice injected with shCTL or shHSF1 cells. Metastatic tumor volume was measured using Living Image 4.7 by measuring the average flux (p/s) for each tumor and calculating the mean for tumors in mice injected with shCTL or shHSF1 cells.

Tissue processing and immunohistochemistry

Mouse leg bone samples were fixed in 4% paraformaldehyde in phosphate buffered saline and decalcified in a 10% EDTA solution followed by embedding, dehydration, and sectioning. Matched primary and metastatic tumor tissue sections were acquired from the Siteman Cancer Center at Washington University in St. Louis. Independent primary and metastatic tumor tissue was acquired commercially from TissueArray.com (BR1141a, MT801, GL861b) as well as additional samples provided by the Indiana University Comprehensive Cancer Center Biospecimen Collection and Banking Core. Commercial samples and institutional samples were de-identified but were collected and used as approved by the Indiana University Institutional Review Board. Tissue underwent immunohistochemistry (IHC) as we have described previously.[17] Antibodies used for IHC included p-HSF1 (S326) (Cell Signaling Technology 4872, RRID: AB_1310328), OC (StressMarq #SPC-507D, RRID:AB_10960639), and HLA-C (Abcam #ab307361, RRID:AB_3675730). Antibodies utilized 10 mmol/L EDTA for antigen retrieval and all slides were counterstained with hematoxylin. After mounting, slides were imaged with Motic EasyScan scanner and analyzed with QuPath software.[58] QuPath analysis of the percentage of cells from each sample that were positive for p-HSF1 (S326) in the nucleus was utilized to determine the threshold for high or low HSF1 active groups. The samples were split at the median for the percentage of cells with nuclear active HSF1, samples above the median were considered high HSF1 active samples, and those below the median were low HSF1 active samples.

Aβ (1-42) peptide transfection and ELISA detection of Aβ fibrils

To transduce Aβ (1–42), cells were plated at 40–60% confluence. After 24 h, 2 μg of Aβ (1-42) (Abcam; ab120301) was transfected into cells using Xfect Protein Transfection kit (Takara Bio 631324) according to manufacturer's protocol. Cells were collected after 8, 18, or 24 h and then processed for downstream applications. To detect the levels of Aβ fibrils, the insoluble fraction of cells was isolated as previously described.[36] Ten micrograms of sonicated detergent-insoluble cell fraction was coated on a high binding 96 well ELISA plate (Santa Cruz, sc-204463), uncovered, and incubated in a 37 °C incubator for overnight until dry. Warmed 1X TBS-T wash buffer was added to dissolve the dried sample and wash the well three times. Blocking was performed using 5% BSA for 1 h at room temperature. Wells were then incubated in primary antibody (OC; StressMarq #SPC-507D; RRID:AB_10960639) at 4 °C

overnight. The next day, rabbit-HRP secondary antibody was added for 2 h at room temperature. Wells were then washed with 1X TBS-T wash buffer before adding warmed 100 uL 1-Step Ultra TMB-ELISA Substrate Solution (Thermo Fisher, #34028) and 1 N HCl was added to stop the reaction. The signal was measured using a plate reader at 450 nm absorption wavelength.

RT-qPCR

Total RNA was isolated using the Micro Total RNA isolation kit (Zymo). RNA was quantified by nanodrop and reverse transcribed using random primers from a reverse transcription kit (Applied Biosystems). Quantitative PCR was performed using a SYBR green master mix (Applied Biosystems) along with gene-specific primers using QuantStudio 3 (Applied Biosystems). Primers used included i) GAPDH forward 5'-CCTGCA CCACCAACTGCTTA-3' and reverse 5'-GGCCATCCA CAGTCTTCTGAG-3' and ii) HSP27 forward 5'-AGCT GACGGTCAAGACCAAG-3' and reverse 5'-GTGAAGC ACCGGGAGATGTA-3'.

Synthesis of I_{HSF1}115

All reactions were performed in flame or oven-dried glassware under an argon atmosphere unless otherwise noted. All commercial reagents were used as received unless otherwise noted. All materials were vacuum dried (1–5 mmHg) to remove trace elements of solvent. "in vacuo" refers to bulk solvent removal, which was performed by a Buchi rotary evaporator linked to a water aspirator. Bulk solvent removal of solvents with boiling points above 80 °C was performed on a Buchi rotary evaporator, which was connected to Precision Scientific vacuum, which allowed for pressures of 1 mmHg. Bulk grade solvents hexanes and ethyl acetate were distilled before use for chromatography. Diethyl ether, tetrahydrofuran, methylene chloride (DCM), 1,2-dichloroethane (DCE), dimethylfomamide, and toluene were dried on a commercial solvent system before use in reactions. Hexamethylphosphoramide and N, N'-dimethylpropyleneurea were both distilled from CaH_2 and stored over 3 Å molecular sieves. Triethylamine, pyridine, and diisopropylethylamine were distilled from CaH_2 under dry argon immediately before use.

Proton nuclear magnetic resonance (^{1}H NMR) spectra and carbon nuclear magnetic resonance (^{13}C NMR) spectra were measured on a Varian VXR (400 MHz), Varian INOVA-400 (400 MHz), Varian INOVA 500 (500 MHz) insturments. H^1 NMR and ^{13}C NMR are reported in parts per million (ppm) downfield from tetramethylsilane and calibrated using residual undeuterated chloroform as an internal standard which is set to δ 7.26. ^{1}H NMR spectra data were reported in the form δ (multiplicity, coupling constants (Hz), integration). Multiplicities are reported as follows: s = singlet, d = doublet, t = triplet, q = quartet, m = multiplet, br = broad, dd = doublet of doublet, dt = doublet of triplet, ABq = AB quartet. Mass spectra data (GCMS, LCMS, HRMS) were recorded on Agilent Technologies 6890 N 15973 (EI), Agilent Technologies 1200 series/6130(ESI), and Waters/Synapt Horns mass spectrometers using chemical ionization (CI) with methane and/or electrospray ionization (ESI).

Analytical thin-layer chromatography was performed using glass-backed 0.25 mm thickness silica gel 60 (F_{254}) plates which were visualized under UV light and/or by staining with ethanolic p-anisaldehyde, potassium permanganate, vanillin, dintrophenylhydrazine, and bromocresol green followed by heating on a hot plate. Iodine crystals were used to develop thin-layer chromatography plates in a glass chamber. Flash chromatography was performed using Merck silica gel 60 (Kiesegel 60) from Whatman Scientific or Sorbent Technologies and pressure was obtained using an in-house airline.

I_{HSF}115 was synthesized according to the previously published method[39] with a modification to the cyclodehydration step to obtain methyl (E)-3-(5,6-dihydro-4H-1,3-oxazin-2-yl)acrylate S2.

Methyl (E)-3-(5,6-dihydro-4H-1,3-oxazin-2-yl)acrylate S2.

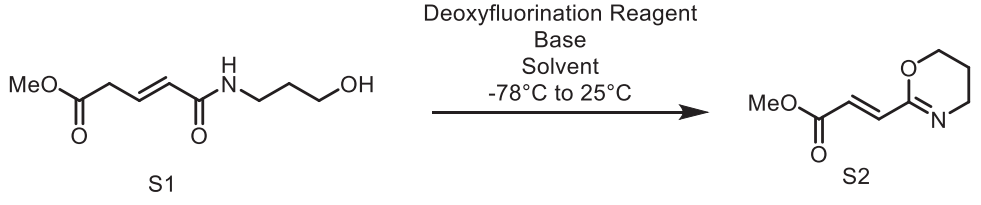

General method for cyclodehydration of γ-hydroxy amide methyl esters with deoxyfluorination reagents

Deoxyfluorination reagent (DAST or XtalFluor-E) (0.2 mmol, 2 eq) was added to a solution of amide S1 in solvent (DCM or DCE) 0.1 M at −78 °C and stirred for 1 h. Base (K_2CO_3 or DBU) (0.2 mmol, 2eq) was then added, and the solution was allowed to warm to 25 °C and stirred at this temperature for 30 min. A saturated aqueous solution of $NaHCO_3$ was then added dropwise and the aqueous layer was extracted 3× with DCM, dried with Na_2SO_4, and concentrated in vacuo. The crude mixture was then purified by silica gel chromatography using 85% ethyl acetate and 15% hexanes to provide **S2** (94–96% yield). Characterized by R_f (100%EtOAc) = 0.31. Spectroscopy is consistent with the literature..

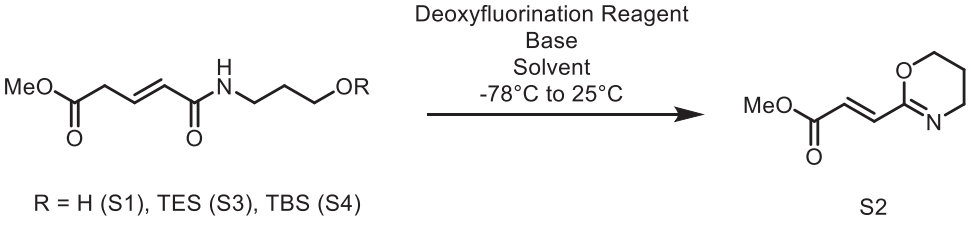

R = H (S1), TES (S3), TBS (S4)

S2

General method for cyclodehydration of silyl protected γ-hydroxy amide methyl esters with deoxyfluorination reagents

Deoxyfluorination reagent (DAST or XtalFluor-E) (0.2 mmol, 2 eq) was added to a solution of amide S3 in solvent (DCM or DCE) 0.1 M at −78 °C and stirred for 1 h. Then the cold bath was removed, and the solution was allowed to warm to 25 °C slowly and stirred for an additional 30 min. A saturated aqueous solution of $NaHCO_3$ was then added dropwise and the aqueous layer was extracted 3× with DCM, dried with Na_2SO_4, and concentrated in vacuo. The crude mixture was then purified by silica gel chromatography using 85% ethyl acetate and 15% hexanes to give S2 (93% yield). Characterized by R_f (100%EtOAc) = 0.31. Spectroscopy is consistent with the literature.

DDQ was added to a stirring solution of PPh_3 (2 g, 8.01 mmol, 1.5 eq) in DCM (50 mL) at 0 °C. The ice bath was removed, and the solution was stirred at 25 °C for 20 min. Hexamethylphosphoramide (0.6 mL) was added dropwise to a suspension of amide S1 (1.074 g, 5.34 mmol, 1 eq) in 6 mL DCM until the solution became homogenous. The solution of the amide was then added dropwise *via* cannula over 10 min at 25 °C then the reaction was stirred for an additional 30 min at 25 °C. The reaction was quenched with 3% aqueous NaOH and the aqueous layer was extracted with DCM (15 mL) 3×. The combined organic layer was then washed 3× with saturated aqueous LiCl, Brine 3×, and DI water 2× then dried with Na_2SO_4 and filtered through a thin pad of celite and concentrated in vacuo. The crude mixture was then purified by silica gel chromatography using 85% ethyl acetate and 15% hexanes to give S2 (68% yield). Characterized by R_f (100%EtOAc) = 0.31. Spectroscopy is consistent with the literature.

CRediT authorship contribution statement **Desmond Jacob:** Validation, Resources, Methodology, Data curation. **Downing Nicholas:** Validation, Investigation, Formal analysis. **Chakrabarti Sunandan:** Validation, Investigation, Formal analysis. **Ray Haimanti:** Validation, Resources, Methodology, Investigation, Formal analysis. **Wang John:** Validation, Methodology, Investigation, Formal analysis, Data curation. **Leriger Gabi:** Validation, Investigation, Formal analysis, Data curation. **Hockaden Natasha:** Writing – review & editing, Writing – original draft, Visualization, Validation, Methodology, Investigation, Formal analysis, Data curation, Conceptualization. **Carpenter Richard L.:** Writing – review & editing, Writing – original draft, Visualization, Supervision, Resources, Project administration, Methodology, Funding acquisition, Formal analysis, Data curation, Conceptualization. **Longmore Gregory:** Writing – review & editing, Resources, Methodology.

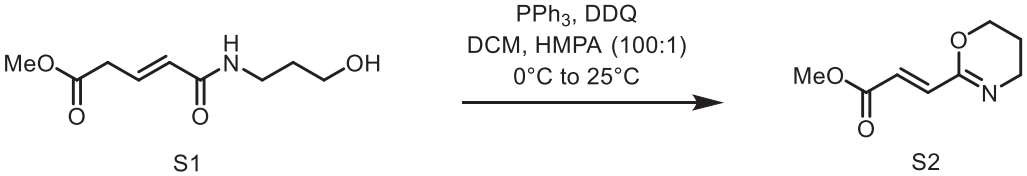

S1

S2

Hollenhorst Peter C.: Writing – review & editing, Supervision, Resources, Methodology, Conceptualization. **Williams David:** Writing – review & editing, Validation, Resources, Methodology, Funding acquisition, Data curation.

Data availability statement Data will be made available on request.

Declarations of interest The authors declare the following financial interests/personal relationships which may be considered as potential competing interests: Richard L. Carpenter reports financial support was provided by National Cancer Institute. David R. Williams reports financial support was provided by National Science Foundation. If there are other authors, they declare that they have no known competing financial interests or personal relationships that could have appeared to influence the work reported in this paper.

Declaration of Generative AI and AI-assisted technologies in the writing process No generative AI tools were used in the writing or editing of this manuscript.

Acknowledgments This work was supported in part by the National Cancer Institute (K22CA207575, RLC), the National Science Foundation (CHE2102587, DRW), and Indiana University (Vice Provost for Research, DRW). We would also like to acknowledge the Indiana University core facilities that made this work possible, including the Laboratory Animal Resources, the Light Microscopy Imaging Center, and the Indiana University School of Medicine Histology Lab.

Appendix A. Supporting information

Supplementary data associated with this article can be found in the online version at doi:10.1016/j.cstres.2025.03.003.

References

1. American Cancer Society. Cancer Facts and Figures 2024. Atlanta, GA; 2024, (https://www.cancer.org/research/cancer-facts-statistics/all-cancer-facts-figures/2024-cancer-facts-figures.html).
2. Giaquinto AN, Sung H, Newman LA, et al. Breast cancer statistics 2024. *CA Cancer J Clin.* 2024;74:477–495. https://doi.org/10.3322/caac.21863
3. Costa RLB, Gradishar WJ. Triple-negative breast cancer: current practice and future directions. *J Oncol Pract.* 2017;13:301–303. https://doi.org/10.1200/jop.2017.023333
4. Leon-Ferre RA, Goetz MP. Advances in systemic therapies for triple negative breast cancer. *BMJ.* 2023;381:e071674. https://doi.org/10.1136/bmj-2022-071674
5. DeSantis CE, Ma J, Gaudet MM, et al. Breast cancer statistics, 2019. *CA Cancer J Clin.* 2019;69:438–451. https://doi.org/10.3322/caac.21583
6. van Zijl F, Krupitza G, Mikulits W. Initial steps of metastasis: cell invasion and endothelial transmigration. *Mutat Res.* 2011;728:23–34. https://doi.org/10.1016/j.mrrev.2011.05.002
7. Jin X, Mu P. Targeting breast cancer metastasis. *Breast Cancer.* 2015;9:23–34. https://doi.org/10.4137/bcbcr.S25460
8. Xie HY, Shao ZM, Li DQ. Tumor microenvironment: driving forces and potential therapeutic targets for breast cancer metastasis. *Chin J Cancer.* 2017;36:36. https://doi.org/10.1186/s40880-017-0202-y
9. Hüsemann Y, Geigl JB, Schubert F, et al. Systemic spread is an early step in breast cancer. *Cancer Cell.* 2008;13:58–68. https://doi.org/10.1016/j.ccr.2007.12.003
10. Luzzi KJ, MacDonald IC, Schmidt EE, et al. Multistep nature of metastatic inefficiency: dormancy of solitary cells after successful extravasation and limited survival of early micrometastases. *Am J Pathol.* 1998;153:865–873. https://doi.org/10.1016/s0002-9440(10)65628-3
11. Kienast Y, von Baumgarten L, Fuhrmann M, et al. Real-time imaging reveals the single steps of brain metastasis formation. *Nat Med.* 2010;16:116–122. https://doi.org/10.1038/nm.2072
12. Gomez-Pastor R, Burchfiel ET, Thiele DJ. Regulation of heat shock transcription factors and their roles in physiology and disease. *Nat Rev Mol Cell Biol.* 2018;19:4–19. https://doi.org/10.1038/nrm.2017.73
13. Carpenter R a YG-P. HSF1 as a cancer biomarker and therapeutic target. *Current Cancer Drug Targets.* 2019;19:515–524. https://doi.org/10.2174/1568009618666181018162117
14. Tang Z, Dai S, He Y, et al. MEK guards proteome stability and inhibits tumor-suppressive amyloidogenesis via HSF1. *Cell.* 2015;160:729–744. https://doi.org/10.1016/j.cell.2015.01.028
15. Carpenter RL, Sirkisoon S, Zhu D, et al. Combined inhibition of AKT and HSF1 suppresses breast cancer stem cells and tumor growth. *Oncotarget.* 2017;8:73947–73963. https://doi.org/10.18632/oncotarget.18166
16. Gökmen-Polar Y, Badve S. Upregulation of HSF1 in estrogen receptor positive breast cancer. *Oncotarget.* 2016;7:84239–84245. https://doi.org/10.18632/oncotarget.12438
17. Jacobs C, Shah S, Lu WC, et al. HSF1 inhibits antitumor immune activity in breast cancer by suppressing CCL5 to block CD8+ T-cell recruitment. *Cancer Res.* 2024;84:276–290. https://doi.org/10.1158/0008-5472.CAN-23-0902
18. Mendillo ML, Santagata S, Koeva M, et al. HSF1 drives a transcriptional program distinct from heat shock to support highly malignant human cancers. *Cell.* 2012;150:549–562. https://doi.org/10.1016/j.cell.2012.06.031
19. Santagata S, Hu R, Lin NU, et al. High levels of nuclear heat-shock factor 1 (HSF1) are associated with poor prognosis in breast cancer. *Proc Natl Acad Sci USA.* 2011;108:18378–18383. https://doi.org/10.1073/pnas.1115031108
20. Eroglu B, Pang J, Jin X, Xi C, Moskophidis D, Mivechi NF. HSF1-mediated control of cellular energy metabolism and mTORC1 activation drive acute T-cell lymphoblastic leukemia progression. *Mol Cancer Res.* 2020;18:463–476. https://doi.org/10.1158/1541-7786.Mcr-19-0217
21. Scherz-Shouval R, Santagata S, Mendillo ML, et al. The reprogramming of tumor stroma by HSF1 is a potent enabler of malignancy. *Cell.* 2014;158:564–578. https://doi.org/10.1016/j.cell.2014.05.045
22. Fujimoto M, Takii R, Takaki E, et al. The HSF1-PARP13-PARP1 complex facilitates DNA repair and promotes mammary tumorigenesis. *Nat Commun.* 2017;8:1638. https://doi.org/10.1038/s41467-017-01807-7
23. Liang W, Liao Y, Zhang J, et al. Heat shock factor 1 inhibits the mitochondrial apoptosis pathway by regulating second mitochondria-derived activator of caspase to promote pancreatic tumorigenesis. *J Exp Clin Cancer Res.* 2017;36:64. https://doi.org/10.1186/s13046-017-0537-x

24. Wang J, He H, Yu L, et al. HSF1 down-regulates XAF1 through transcriptional regulation. *J Biol Chem.* 2006;281:2451–2459. https://doi.org/10.1074/jbc.M505890200
25. Carpenter RL, Paw I, Dewhirst MW, Lo HW. Akt phosphorylates and activates HSF-1 independent of heat shock, leading to Slug overexpression and epithelial-mesenchymal transition (EMT) of HER2-overexpressing breast cancer cells. *Oncogene.* 2015;34:546–557. https://doi.org/10.1038/onc.2013.582
26. Chen K, Qian W, Li J, et al. Loss of AMPK activation promotes the invasion and metastasis of pancreatic cancer through an HSF1-dependent pathway. *Mol Oncol.* 2017;11:1475–1492. https://doi.org/10.1002/1878-0261.12116
27. Huang M, Dong W, Xie R, et al. HSF1 facilitates the multistep process of lymphatic metastasis in bladder cancer via a novel PRMT5-WDR5-dependent transcriptional program. *Cancer Commun.* 2022;42:447–470. https://doi.org/10.1002/cac2.12284
28. Powell CD, Paullin TR, Aoisa C, Menzie CJ, Ubaldini A, Westerheide SD. The heat shock transcription factor HSF1 induces ovarian cancer epithelial-mesenchymal transition in a 3D spheroid growth model. *PLoS One.* 2016;11:e0168389. https://doi.org/10.1371/journal.pone.0168389
29. Xi C, Hu Y, Buckhaults P, Moskophidis D, Mivechi NF. Heat shock factor Hsf1 cooperates with ErbB2 (Her2/Neu) protein to promote mammary tumorigenesis and metastasis. *J Biol Chem.* 2012;287:35646–35657. https://doi.org/10.1074/jbc.M112.377481
30. Khaleque MA, Bharti A, Sawyer D, et al. Induction of heat shock proteins by heregulin beta1 leads to protection from apoptosis and anchorage-independent growth. *Oncogene.* 2005;24:6564–6573. https://doi.org/10.1038/sj.onc.1208798
31. Meng L, Gabai VL, Sherman MY. Heat-shock transcription factor HSF1 has a critical role in human epidermal growth factor receptor-2-induced cellular transformation and tumorigenesis. *Oncogene.* 2010;29:5204–5213. https://doi.org/10.1038/onc.2010.277
32. Bartha Á, Győrffy B. TNMplot.com: a web tool for the comparison of gene expression in normal, tumor and metastatic tissues. *Int J Mol Sci.* 2021;22:2622. https://doi.org/10.3390/ijms22052622
33. Kang Y, Siegel PM, Shu W, et al. A multigenic program mediating breast cancer metastasis to bone. *Cancer Cell.* 2003;3:537–549. https://doi.org/10.1016/s1535-6108(03)00132-6
34. Lee YJ, Kim EH, Lee JS, et al. HSF1 as a mitotic regulator: phosphorylation of HSF1 by Plk1 is essential for mitotic progression. *Cancer Res.* 2008;68:7550–7560. https://doi.org/10.1158/0008-5472.Can-08-0129
35. Kayed R, Head E, Sarsoza F, et al. Fibril specific, conformation dependent antibodies recognize a generic epitope common to amyloid fibrils and fibrillar oligomers that is absent in prefibrillar oligomers. *Mol Neurodegener.* 2007;2:18. https://doi.org/10.1186/1750-1326-2-18
36. Tang Z, Su KH, Xu M, Dai C. HSF1 physically neutralizes amyloid oligomers to empower overgrowth and bestow neuroprotection. *Sci Adv.* 2020;6. https://doi.org/10.1126/sciadv.abc6871
37. Dong B, Jaeger AM, Hughes PF, et al. Targeting therapy-resistant prostate cancer via a direct inhibitor of the human heat shock transcription factor 1. *Sci Transl Med.* 2020;12. https://doi.org/10.1126/scitranslmed.abb5647
38. Yoon YJ, Kim JA, Shin KD, et al. KRIBB11 inhibits HSP70 synthesis through inhibition of heat shock factor 1 function by impairing the recruitment of positive transcription elongation factor b to the hsp70 promoter. *J Biol Chem.* 2011;286:1737–1747. https://doi.org/10.1074/jbc.M110.179440
39. Vilaboa N, Bore A, Martin-Saavedra F, et al. New inhibitor targeting human transcription factor HSF1: effects on the heat shock response and tumor cell survival. *Nucleic Acids Res.* 2017;45:5797–5817. https://doi.org/10.1093/nar/gkx194
40. Edmondson R, Broglie JJ, Adcock AF, Yang L. Three-dimensional cell culture systems and their applications in drug discovery and cell-based biosensors. *Assay Drug Dev Technol.* 2014;12:207–218. https://doi.org/10.1089/adt.2014.573
41. Dong Q, Xiu Y, Wang Y, et al. HSF1 is a driver of leukemia stem cell self-renewal in acute myeloid leukemia. *Nat Commun.* 2022;13:6107. https://doi.org/10.1038/s41467-022-33861-1
42. Im CN, Yun HH, Lee JH. Heat shock factor 1 depletion sensitizes A172 glioblastoma cells to temozolomide via suppression of cancer stem cell-like properties. *Int J Mol Sci.* 2017;18. https://doi.org/10.3390/ijms18020468
43. Kusumoto H, Hirohashi Y, Nishizawa S, et al. Cellular stress induces cancer stem-like cells through expression of DNAJB8 by activation of heat shock factor 1. *Cancer Sci.* 2018;109:741–750. https://doi.org/10.1111/cas.13501
44. Qin T, Chen K, Li J, et al. Heat shock factor 1 inhibition sensitizes pancreatic cancer to gemcitabine via the suppression of cancer stem cell-like properties. *Biomed Pharmacother.* 2022;148:112713. https://doi.org/10.1016/j.biopha.2022.112713
45. Shi Y, Sun L, Zhang R, et al. Thrombospondin 4/integrin α2/HSF1 axis promotes proliferation and cancer stem-like traits of gallbladder cancer by enhancing reciprocal crosstalk between cancer-associated fibroblasts and tumor cells. *J Exp Clin Cancer Res.* 2021;40:14. https://doi.org/10.1186/s13046-020-01812-7
46. Wang B, Lee CW, Witt A, Thakkar A, Ince TA. Heat shock factor 1 induces cancer stem cell phenotype in breast cancer cell lines. *Breast Cancer Res Treat.* 2015;153:57–66. https://doi.org/10.1007/s10549-015-3521-1
47. Yasuda K, Hirohashi Y, Mariya T, et al. Phosphorylation of HSF1 at serine 326 residue is related to the maintenance of gynecologic cancer stem cells through expression of HSP27. *Oncotarget.* 2017;8:31540–31553. https://doi.org/10.18632/oncotarget.16361
48. Hoj JP, Mayro B, Pendergast AM. The ABL2 kinase regulates an HSF1-dependent transcriptional program required for lung adenocarcinoma brain metastasis. *Proc Natl Acad Sci U S A.* 2020;117:33486–33495. https://doi.org/10.1073/pnas.2007991117
49. Dai C, Sampson SB. HSF1: guardian of proteostasis in cancer. *Trends Cell Biol.* 2016;26:17–28. https://doi.org/10.1016/j.tcb.2015.10.011
50. Smith RS, Takagishi SR, Amici DR, et al. HSF2 cooperates with HSF1 to drive a transcriptional program critical for the malignant state. *Sci Adv.* 2022;8:eabj6526. https://doi.org/10.1126/sciadv.abj6526
51. Dakal TC, Bhushan R, Xu C, et al. Intricate relationship between cancer stemness, metastasis, and drug resistance. *MedComm.* 2024;5:e710. https://doi.org/10.1002/mco2.710
52. Lambert AW, Weinberg RA. Linking EMT programmes to normal and neoplastic epithelial stem cells. *Nat Rev Cancer.* 2021;21:325–338. https://doi.org/10.1038/s41568-021-00332-6
53. Cheeseman MD, Chessum NE, Rye CS, et al. Discovery of a chemical probe bisamide (CCT251236): an orally bioavailable efficacious pirin ligand from a heat shock transcription factor 1 (HSF1) phenotypic screen. *J Med Chem.* 2017;60:180–201. https://doi.org/10.1021/acs.jmedchem.6b01055

54. Pasqua AE, Sharp SY, Chessum NEA, et al. HSF1 pathway inhibitor clinical candidate (CCT361814/NXP800) developed from a phenotypic screen as a potential treatment for refractory ovarian cancer and other malignancies. *J Med Chem.* 2023;66:5907–5936. https://doi.org/10.1021/acs.jmedchem.3c00156
55. Powers MV, Sharp SY, Lampraki E-M, et al. Abstract LB234: activation of the integrated stress response by the developmental HSF1 pathway inhibitor NXP800. *Cancer Research.* 2023;83:LB234. https://doi.org/10.1158/1538-7445.Am2023-lb234
56. Bos PD, Zhang XHF, Nadal C, et al. Genes that mediate breast cancer metastasis to the brain. *Nature.* 2009;459:1005–1009. https://doi.org/10.1038/nature08021
57. Lu WC, Omari R, Ray H, et al. AKT1 mediates multiple phosphorylation events that functionally promote HSF1 activation. *FEBS J.* 2022;289:3876–3893. https://doi.org/10.1111/febs.16375
58. Bankhead P, Loughrey MB, Fernandez JA, et al. QuPath: open source software for digital pathology image analysis. *Sci Rep.* 2017;7:16878. https://doi.org/10.1038/s41598-017-17204-5